JOURNAL OF MATERIALS SCIENCE 25 (1990) 1997–2003

A case for Taylor hardening during primary and steady-state creep in aluminium and type 304 stainless steel

M. E. KASSNER
Lawrence Livermore National Laboratory. PO Box 808, L-355, Livermore, California 94550, USA

Previous elevated-temperature experiments on 304 stainless steel clearly show that the density of dislocations within the subgrain interior influences the flow stress at a given strain rate and temperature. A re-evaluation shows that the hardening is consistent with the Taylor relation if a linear superposition of solute hardening (τ_0, or the stress necessary to cause dislocation motion in the absence of a dislocation substructure) and dislocation ($\alpha G\mathbf{b}\varrho^{1/2}$) hardening is assumed. The same Taylor relation is applicable to steady-state structures of aluminium if the yield stress of annealed aluminium is assumed equal to τ_0. New tests on aluminium deforming under constant-strain-rate creep conditions show a monotonic increase in the dislocation density with strain. This and the constant-stress creep trends are shown to be possibly consistent with Taylor hardening.

1. Introduction

Most theories for five-power-law creep ($T > 0.6\,T_m$, where T_m is the melting temperature) of pure metals and Class II alloys rely upon some aspect of the subgrain substructure to describe the rate-controlling process. Many of the more recent theories rely upon the details of the subgrain boundaries such as the spacing, d, of dislocations that compose the boundaries (related to the misorientation angle, θ, across boundaries) [1–9] and/or the subgrain size, λ [10]. The dislocations not associated with the subgrain boundaries, which can form a Frank network, are less commonly associated with the rate-controlling process of five-power-law creep. Dislocation network theories [11–16] generally suppose that the creep behaviour is explained in terms of network coarsening (diffusion-controlled) and the activation of critical-size links in the network into sources of gliding dislocations. The network-based theories have been refined in recent years [13, 16] although acceptance has been relatively limited.

This is perhaps somewhat unjustified in view of some more recent experiments. For example, experiments under power-law or near-power-law conditions show that there is really no doubt now that the elevated-temperature flow stress of 304 stainless steel, a Class II alloy, is controlled by the density (ϱ) of dislocations not associated with subgrain boundaries (network dislocations) [17–21]. Perhaps more interestingly, recent experiments have also shown that the flow properties of aluminium (under five-power-law conditions) appear independent of the subgrain size and the misorientation angle across subgrain boundaries [22, 23]. Power-law creep in aluminium has been both traditionally and more recently associated with subgrains [4, 5, 24–29]. Of course, if a particular feature (d, λ, or ϱ) is associated with the rate-controlling process for five-power-law creep, then the yield stress at a fixed T and strain rate $\dot{\varepsilon}$ (within the power-law range) would be expected to be a function of the dimensions of this (rather than another) feature.

This paper has two parts. First, a re-evaluation of the earlier 304 stainless steel experiments by the author [17] will show that the influence of dislocation density on the flow stress is consistent with the Taylor equation:

$$\tau|_{T,\dot{\varepsilon}} = \tau_0 + \alpha G\mathbf{b}\varrho^{1/2} \quad (1)$$

where $\tau|_{T,\dot{\varepsilon}}$ is the applied shear stress at a given temperature and strain rate, G is the shear modulus, $\mathbf{b}$ is the Burger's vector, α is a constant that has been experimentally found to be roughly 0.5 [30], and τ_0 is the stress required to move a dislocation in the absence of other dislocations that can arise as a result of solutes or a Peierls-type stress. This equation was shown to describe reasonably 304 data by assuming that τ_0 is approximately equal to the yield stress of the annealed alloy. Furthermore, analysis will show that the flow stress of aluminium (with various steady-state or stage II creep microstructures) at a given temperature and strain also obeys Equation 1.

Second, special tests were performed in this research to establish the trends of dislocation density against strain in aluminium deforming at elevated temperature under constant-strain-rate conditions. It will be shown that the microstructure and flow characteristics of aluminium undergoing primary (or Stage I) creep under *either* constant-stress or constant-strain-

0022–2461/90 $03.00 + .12 © *1990 Chapman and Hall Ltd.*

rate power-law creep conditions are not inconsistent with Taylor hardening.

2. Experimental procedure

The aluminium used in this study was of 99.999% purity. Solid specimens were torsionally deformed to primary and steady-state creep strains under constant-strain-rate conditions and were water-quenched immediately after deformation. The specimens were then prepared for examination by transmission electron microscopy. In this study the dislocation density was measured in a manner identical to that of an earlier study by the author [23], except that the grinding step was eliminated. Although these previous sample-preparation techniques were reliable for measurements of λ and misorientation angle θ, they may have been slightly inaccurate for ϱ determinations because of the grinding step (possibly a 10–20% overestimation in ϱ). Thick sections were cut from the surface of the quenched torsion specimens using a 0.15-mm thick diamond blade. The sections were then jet-polished to perforation without involving a grinding step. Fifty TEM micrographs were taken at each strain level and an average density of dislocations not associated with subgrain boundaries was determined.

3. Analysis and results

In earlier work, the author [17, 18] specially prepared specimens of 304 stainless steel having various combinations of λ and ϱ microstructures by utilizing a variety of thermal and mechanical treatments. The specimens were mechanically tested at a given temperature and strain rate that nearly corresponded to the five-power-law creep range. It was found that the dislocation density rather than the subgrain size dominated the strength. The flow stress was originally described by a root-mean-square (r.m.s.) equation into which solute strengthening and λ and ϱ values could be substituted. Both the reciprocal subgrain size and ϱ terms of the r.m.s. equation were raised to exponents of 0.24. Alternately, the strength-predicting equation could take the form of Equation 1 with only a minor loss (if any) of predictive capability [17]. Furthermore, it might be argued that the superposition of solute and dislocation hardening should follow a linear rather than r.m.s. form [31]. Figure 1 plots the yield strength at 750° C (0.57 T_m) and $\dot{\gamma} = 9.6 \times 10^{-4}\,\text{sec}^{-1}$. The data can clearly be described by an equation that is consistent with Equation 1:

$$\tau|_{750°\text{C},\ 9.6\times10^{-4}\text{sec}^{-1}} = \tau_{y(\text{annealed})} + \alpha G\mathbf{b}\varrho^{1/2} \qquad (2)$$

Furthermore, $\alpha \simeq 0.49$, which is consistent with observed values for Taylor hardening. An important point here is that for a given dislocation density, the flow stress is nearly *independent* of λ since, as discussed in the earlier work [17], there is only a small increase in the strength by subgrain refinement at a given ϱ. The r.m.s. equation that described the data of Fig. 1 also accurately predicted the Stage I flow for 304 stainless steel at 0.63 and 0.74 T_m based on the microstructures observed at various primary creep strains at each temperature. This, of course, suggested that

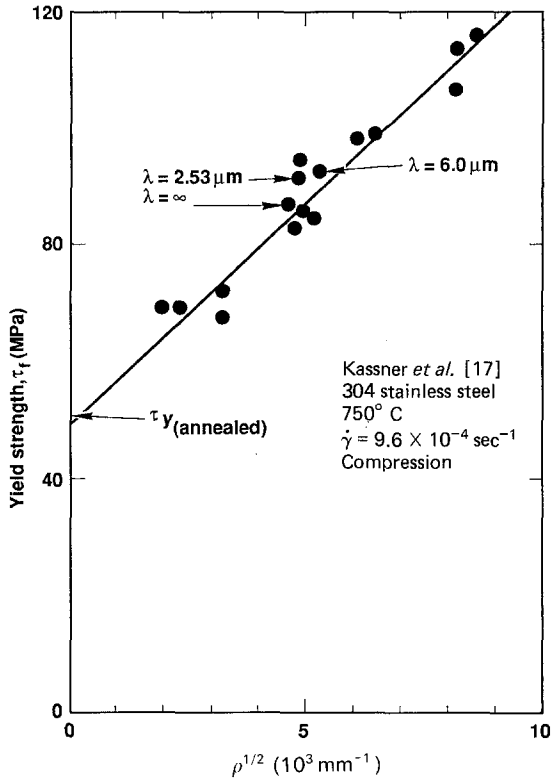

Figure 1 The elevated-temperature flow stress of 304 stainless steel is plotted as a function of the square root of the dislocation density. Note that the flow stress is relatively insensitive to dramatic changes in the subgrain size.

Equation 2 is valid at temperatures well above 0.57 T_m. It should perhaps be mentioned that the *steady-state* flow stress σ_{ss} has been conventionally [1, 32, 33] related to the steady-state dislocation density ϱ_{ss} by

$$(\sigma/E)_{ss} = K\varrho_{ss}^{1/2} \qquad (3)$$

where K is a constant and E is Young's modulus. However, this is an artificial Taylor relationship since the steady-state stresses are associated with different temperatures and/or strain rates, rather than fixed values as in Equation 1.

The kind of experiment illustrated by Fig. 1 has also been performed on steady-state creep structures of aluminium [25, 28]. In one case [28], aluminium specimens were deformed to various steady-state stresses at a given temperature by varying the applied strain rate. The strain rate was very quickly changed to a common rate after steady state was achieved and the new plastic-flow (yield) stress (σ_y) was noted. The subgrain sizes were measured at each steady state, so that the dependence of the flow stress at a specific temperature and strain rate on the subgrain size could be determined. The data of Young *et al.* [28] is shown in Fig. 2. The data shows that at 450° C (0.77 T_m), smaller subgrain sizes are associated with higher strength. Similarly, Kikuchi and Yamaguchi [25] deformed three specimens at various temperatures and strain rates, again to steady state. The specimens were then quickly cooled at 300° C and re-deformed at a fixed strain rate. The new flow stresses are also related to the measured (steady-state) subgrain sizes produced at the higher temperatures in Fig. 2. The

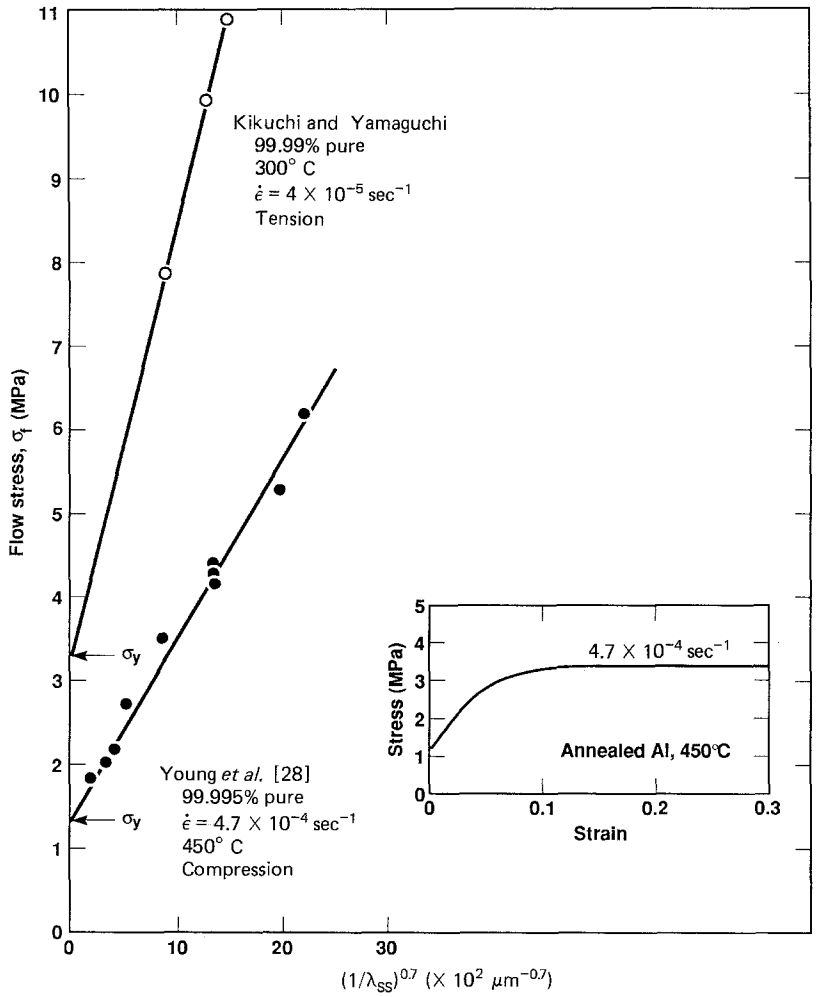

Figure 2 The flow stress of steady-state-substructure aluminium is plotted as a function of the reciprocal (steady-state) subgrain size raised to the 0.7 power for two elevated temperatures. The inset shows the stress–strain behaviour of annealed aluminium at temperature and strain-rate conditions identical to one set of the plotted data.

inset shows the stress-strain behaviour of annealed aluminium at 450° C. Note that for the annealed material ($\lambda = \infty$, and ϱ is relatively low) the yield stress is a substantial fraction (0.35) of the steady-state stress. This means that, as with Equation 1, we need to consider the stress σ_0 necessary for yielding in the absence of a dislocation substructure, which is assumed nearly equal to the yield stress of annealed aluminium. This suggests a simple relationship to describe the data of Fig. 2:

$$\sigma_f|_{T,\dot{\varepsilon}} = \sigma_0 + k_1(1/\lambda_{ss})^{0.7} \quad (4)$$

where k_1 is a constant. Young *et al.* [28] suggested an alternative equation that did not include a σ_0 term:

$$\sigma_f|_{T,\dot{\varepsilon}} = k_2(1/\lambda_{ss})^{0.29} \quad (5)$$

It was later suggested that exponents of roughly this value ($\simeq 0.40$) may be valid for a variety of materials [10]. The reciprocal subgrain size exponent is lower than that of Equation 4 because the σ_0 term was not considered, which, as the Fig. 2 inset (as well as Fig. 5) shows, is probably necessary. The explanation for the fact that the k_1 values for the two studies of Fig. 2 are different is not readily apparent. The value k_1 may be temperature-dependent or there may be a systematic overestimation of subgrain sizes by Kikuchi and Yamaguchi [25]. The latter possibility is based on comparison of their values of λ with other strudies [34] at comparable steady-state stress levels.

Equation 4 was based on data from steady-state structures. Since the steady-state subgrain size generally is directly related to the steady-state dislocation density, ϱ_{ss}, in the subgrain interiors, we can relate $\sigma_f|_{T,\dot{\varepsilon}}$ in Equation 4 to ϱ_{ss}. Generally, it has been found that [32–34]:

$$(\sigma/E)_{ss} = K'(1/\lambda_{ss}) \quad (6)$$

where K' is a constant. Again, Equation 6 should not be confused with Equations 4 and 5, since the latter two predict strength at a *specific* T, $\dot{\varepsilon}$ for various subgrain sizes, while the former relates changes in the steady-state flow stress (*different* temperatures and strain rates) to changes in λ_{ss}. It has also been found that:

$$(\sigma/E)^l_{ss} = K''(\varrho_{ss}) \quad (7)$$

where, as pointed out by Takeuchi and Argon [33], l varies between 1 and 2. Substituting Equation 7 into Equation 6 provides a relationship between ϱ_{ss} and λ_{ss} and hence the desired relationship between $\sigma_f|_{T,\dot{\varepsilon}}$ and ϱ_{ss}. Classically, l has been assigned a value of 2 (see [7, 24, 32, 35, 36]), perhaps partly because the equation reduces to Equation 3 which, as mentioned earlier, has (artificial) palatability in terms of the Taylor equation. In reality, l may not be equal to 2. A few experiments

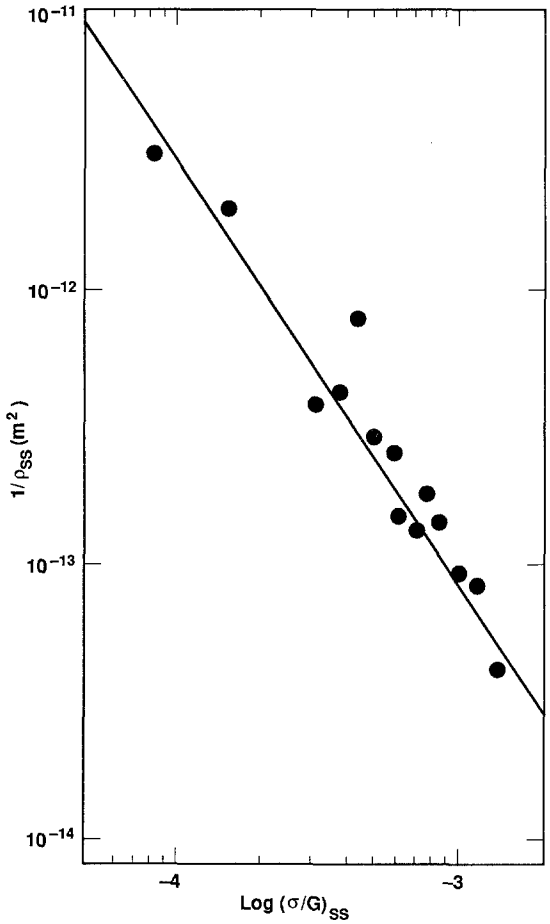

Figure 3 The reciprocal (steady-state) dislocation density is plotted as a function of the modulus-compensated steady-state. The data is that of Blum *et al.* [24] for aluminium. The slope of the line is about 1.57.

have been performed on aluminium to establish l [24, 36]. The data of Blum and co-workers [24], shown in Fig. 3, was based on TEM. The best-fit line suggests that $l \simeq 1.57$ rather than 2. The data of Daily and Ahlquist (etch pit) [36] as plotted by [33] suggests a value of 1.68. If an average value of 1.62 is used, then Equation 4 can be rewritten:

$$\sigma_f|_{T,\dot{\varepsilon}} = \sigma_0 + k_3(\varrho_{ss})^{0.43} \quad (8)$$

where σ_0 is the yield stress of the annealed aluminium at T, $\dot{\varepsilon}$.

There may be an important similarity between Equation 8 and Equation 1. It appears that the phenomenological relationship between the flow stress at a given strain rate and temperature ($\sigma_f|_{T,\dot{\varepsilon}}$) that was based on the observed subgrain sizes of steady-state structures (λ_{ss}) may genuinely reduce to a relationship close to the Taylor equation. We can express the data by an equation of form identical to Equation 1 if we assume the dislocation density exponent in Equation 8 is equal to 0.5. Using the data of Kassner and McMahon [23] as well as [24, 28], α was calculated as between 0.21 and 0.88 or roughly 0.55, again in agreement with the observed values of other materials known to harden by increased dislocation density. Therefore, the phenomenology of the microstructural hardening of steady-state structures of aluminium at elevated temperature, which is usually expressed in terms of subgrain sizes, can be reasonably described by the classic Taylor hardening relationship.

Challenges to the proposition of Taylor hardening include the microstructural observations during primary creep under constant-strain-rate and constant-stress conditions. For example, it has nearly always been observed during primary (Stage I) creep of pure metals and Class II alloys under constant-stress conditions that the density of dislocations not associated with subgrain boundaries increases from the annealed value to a peak value, but then gradually decreases to a steady-state value that is between the annealed and the peak density (aluminium, [24, 36]; 304 stainless steel, [35]). Typically, the peak value, ϱ_p, measured at a strain level that is roughly one-fourth or so of the strain required to attain steady state ($\varepsilon_{ss}/4$), is higher by a factor of 1.5–4 [24, 35–39] than the steady-state ϱ_{ss} value. This behaviour could be interpreted as evidence for these dislocations having a dynamical role rather than a (Taylor) hardening role, since the high initial strain rates in a constant-stress test may require, by the equation

$$\dot{\varepsilon} = k_4 \varrho_m v \mathbf{b} \quad (9)$$

a high mobile (non-hardening) dislocation density, ϱ_m, that gives rise to a high initial value of total density of dislocations not associated with subgrain boundaries, ϱ (v is the dislocation velocity). As steady state is achieved and the strain rate decreases, so does ϱ_m and in turn ϱ. It was believed difficult to rationalize hardening by "forest" dislocations if the overall density is decreasing while the strain rate is decreasing. Therefore, an important question is whether the Taylor hardening perhaps observed in steady-state structure is consistent with the above.

The trends in dislocation density during primary creep have been less completely investigated for the case of constant-strain-rate tests. Earlier work by the author [17] on 304 stainless steel found that at $0.57T_m$ the increase in flow stress by a factor of 3 is associated with increases in dislocation density with strain that are consistent with Equation 2. The author's data at $0.63\,T_m$ [18] is shown in Fig. 4. A peak density during primary creep is not observed in the constant-strain-rate case, here or at $0.57\,T_m$. Rather, it appears that the dislocation density monotonically increases to the steady-state value. As mentioned earlier, the ϱ against ε trends and a microstructurally based equation in which a dislocation-hardening term dominates accurately model the observed stress–strain curve here as well as at $0.57\,T_m$.

This study attempted to establish the ϱ–ε trends in constant-strain-rate tests in aluminium at elevated temperature. In particular, 371° C and a strain rate of $5.04 \times 10^{-4}\,sec^{-1}$ were chosen (five-power-law conditions). It would then be determined whether dislocation hardening alone could rationalize these trends as well as the established constant-stress trends. Earlier work by the author established preliminary ϱ–ε trends in aluminium deformed at a constant strain rate at $0.69\,T_m$ [23]. Although the sample-preparation techniques that were utilized [23] were reliable for λ and θ measurements, they may have been slightly inaccurate for ϱ determinations because of a grinding step (possibly a 10–20% overestimation). In this

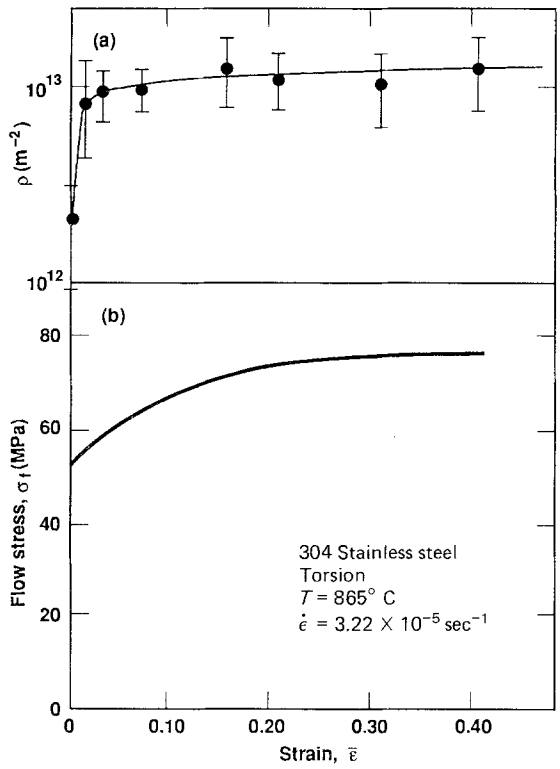

Figure 4 (a) The dislocation density in the subgrain interior against strain, and (b) the stress against strain behaviour of 304 stainless steel deforming under constant-strain-rate conditions at 865° C. Data is from Kassner *et al.* [18].

study, ϱ was measured in essentially an identical manner except that the grinding step was eliminated. The data of this and the previous study are shown in Fig. 5. The stress–strain curves show, as does the inset of Fig. 2, a non-negligible flow stress in the absence of a dislocation substructure (53% of the steady-state stress here). The current and previous dislocation density measurements are in close agreement. The bracket in Fig. 5 at strains above 0.20 is the range of average densities observed at nine strain levels within steady state [23]. Also, the ϱ–ε trends here are similar to those of the stainless steel, where presence of forest dislocation hardening is fairly convincing.

Taylor hardening may be occurring here despite only a modest increase in ϱ (55%, based on ϱ at $\varepsilon_p = 0.03$) to steady state. The argument for Taylor hardening is made in the following. From Equation 9:

$$\dot{\varepsilon} = k_4 \varrho_m v \mathbf{b}$$

We assume [40, 41]

$$v = k_5 \sigma^1 \tag{10}$$

and therefore for constant-strain-rate tests:

$$\dot{\varepsilon} = k_4 k_5 \varrho_m \mathbf{b} \sigma \quad \text{(constant strain rate)} \tag{11}$$

At yielding, ε_p (plastic strain) is small, there is minor hardening, and the mobile dislocation density is approximately equal to the total density:

$$\varrho_{(\varepsilon_p \simeq 0)} \simeq \varrho_{m(\varepsilon_p \simeq 0)}$$

therefore,

$$\varrho_{m(\varepsilon_p \simeq 0)} \simeq 0.64 \varrho_{ss} \quad \text{(based on } \varrho \text{ at } \varepsilon_p = 0.03)$$

Also, from Fig. 5, $\sigma_y/\sigma_{ss} \simeq 0.53$. Therefore, at small strains,

$$\dot{\varepsilon} = k_4 k_5 0.34 \sigma_{ss} \varrho_{ss} \mathbf{b}$$

$$\text{(constant strain rate at } \varepsilon_p \simeq 0.03) \tag{12}$$

At steady state, $\sigma = \sigma_{ssd}$ and $\varrho_m = f_m \varrho_{ss}$, where f_m is the fraction of the total dislocation density that is mobile, and

$$\dot{\varepsilon}_{ss} = k_4 k_5 f_m \varrho_{ss} \sigma_{ss} \mathbf{b}$$

$$\text{(constant strain rate at } \varepsilon_p > 0.20) \tag{13}$$

By combining Equations 12 and 13, we find that f_m at steady state is equal to about 1/3. This suggests that during steady state only 1/3 of the dislocations are mobile and the remaining 2/3 participate in hardening. The finding that a large fraction are immobile is consistent with the observation that increased dislocation density is associated with increased strength (Equation 8). Of course, there is the assumption that the stress acting on dislocations as a function of strain (microstructure) is proportional to the applied flow stress. Furthermore, we have presumed a 55% increase in ϱ over primary creep. Although this is similar to the 304 stainless steel findings, there remains uncertainty in the ϱ determinations here. These two points certainly delineate the tentative nature of the calculation of f_m.

For the constant-stress case we again assume that $\varrho_m \simeq \varrho$ at $\varepsilon_p \simeq 0$ and:

$$\dot{\varepsilon}_{(\varepsilon_p \simeq 0)} = k_4 \varrho_{(\varepsilon_p \simeq 0)} k_5 \sigma_{ss} \mathbf{b} \quad \text{(constant stress)}$$

or

$$\dot{\varepsilon}_{(\varepsilon_p \simeq 0)} = k_4 k_5 \varrho_p \sigma_{ss} \mathbf{b} \tag{14}$$

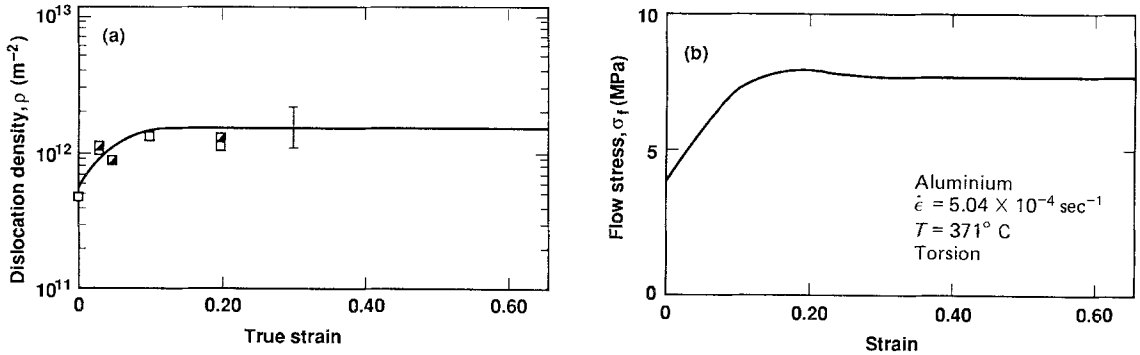

Figure 5 (a) Dislocation density in the subgrain interior against strain (□) Ref. [23] and (◪) this work; and (b) stress against strain for aluminium deforming under constant-strain-rate conditions at 371° C.

where ϱ_p is the peak dislocation density, which will be assumed equal to the maximum dislocation density experimentally observed in a ϱ–ε plot of a constant-stress test. Since, at steady state,

$$\dot{\varepsilon}_{ss} \simeq k_4 k_5 (\varrho_{ss}/3)\sigma_{ss}\mathbf{b}$$

then

$$\dot{\varepsilon}_{\varepsilon_p \simeq 0}/\dot{\varepsilon}_{ss} \simeq 3\varrho_p/\varrho_{ss} \quad \text{(constant stress)} \qquad (15)$$

Though the assumptions have been quite simple, Equation 15 is still interesting because it suggests that fractional decreases in $\dot{\varepsilon}$ in a constant-stress creep test are not equal to those of ϱ. This apparent contradiction to purely dynamical theories (i.e., Equation 9) is reflected in experiments [24, 36–38] where the kind of trend predicted in Equation 15 is observed. The observations of $\dot{\varepsilon}$ against ε in a constant-stress test at the identical temperature can be used to predict roughly the ϱ–ε curve in aluminium at 371°C and about 7.8 MPa. If we use small plastic strain levels (e.g. $\varepsilon \simeq \varepsilon_{ss}/4$ where ϱ values have been measured) we can determine for aluminium an average value of the ratio $[\dot{\varepsilon}_{\varepsilon_p=(\varepsilon_{ss}/4)}/\dot{\varepsilon}_{\varepsilon_p=\varepsilon_{ss}}]$ in a constant-stress test. This value seems to be roughly 6 at stresses and temperatures comparable to the present study [14, 24, 27, 36, 42]. This ratio was applied to Equation 15; the estimated ϱ–ε trends are shown in Fig. 6. This estimate, which predicts a peak dislocation density of 2.0 ϱ_{ss}, is consistent with the general observation mentioned earlier for pure metals and Class II alloys that ϱ_p has been found to be between 1.5 and 4 ϱ_{ss} (1.5–2.0 for aluminium [24, 36]).

It should, perhaps, be mentioned that other explanations of the primary creep ϱ and $\dot{\varepsilon}$ behaviour curves have been made. For example, Barrett *et al.* [43], who assumed that all dislocations within the subgrains are mobile, suggested that the dislocation velocity must *decrease* during a constant-stress test in Fe–3% Si to be consistent with experimental determinations of ϱ and Equation 9. The decrease in v compensates for a decrease in $\dot{\varepsilon}$ that is larger by a factor of 2 than the decrease in ϱ (a decrease in v is not necessary according to Equation 15). Although an explanation for changes in v was not given, a similar claim might be made for constant-stress creep test of aluminium. Furthermore, and perhaps consistently, it might be suggested that v is clearly independent of ε (rather than increasing with ε) in a constant-strain-rate test. If these propositions could be accepted, then the observed data could be argued to be equally consistent with a purely dynamical role for dislocations.

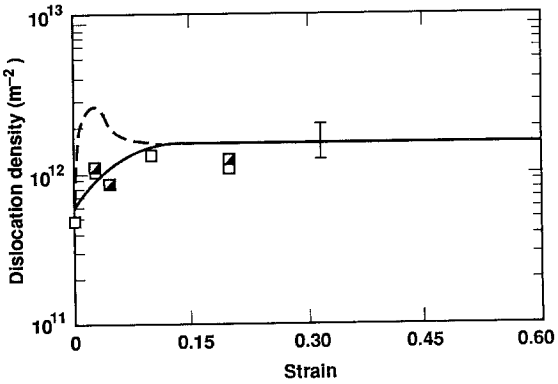

Figure 6 The predicted dislocation density (– – –) in the subgrain interior against strain for aluminium deforming under constant-stress conditions is compared with that for constant-strain-rate conditions (——) at 371°C. (□) Ref. [23] and (◪) this work. The predicted dislocation density is based on Equation 15, which assumes Taylor hardening.

4. Summary

It has been established in earlier work by the author that dislocation hardening accounts for elevated-temperature strength of both primary and steady-state creep microstructures of 304 stainless steel. It was shown here that the dislocation strengthening is consistent with the Taylor law if a realistic "friction" stress is utilized. Furthermore, if a realistic friction stress is again considered, the phenomenological relationship between ϱ_{ss} and λ_{ss} of aluminium can be utilized to show that the flow stress of aluminium at a fixed T and $\dot{\varepsilon}$ obeys a Taylor-like equation. Whereas network dislocations may dominate the microstructure during steady state, mobile dislocations within the subgrain interior compose the majority of dislocations during early primary creep. As a result, "peak" dislocation densities are observed during primary creep under constant-stress conditions. Furthermore, the interior dislocation density increases only modestly during primary creep under constant-strain-rate conditions. Both of these dynamical manifestations, however, are not inconsistent with hardening due to network refinement.

Acknowledgements

This work was performed under the auspices of the US Department of Energy by the Lawrence Livermore National Laboratory under Contract W-7405-Eng-48. The author wishes to thank M. A. Wall for help with the transmission electron microscopy.

References

1. L. BENDERSKY, A. ROSEN and A. K. MUKHERJEE, *Int. Met. Rev.* **30** (1985) 1.
2. W. BLUM, *Phys. Status Solidi* **45** (1971) 561.
3. J. WEERTMAN, "Creep and Fracture of Engineering Materials and Structures," (Pineridge, Swansea, 1984) p. 1.
4. M. A. MORRIS and J. L. MARTIN, *Acta Metall.* **32** (1984) 1609.
5. *Idem, ibid.* **32** (1984) 549.
6. K. MARUYAMA, S. KARASHIMA and H. OIKAWA, *Res. Mechanica* **7** (1983) 21.
7. W. D. NIX and B. ILSCHNER, in "Strength of Metals and Alloys," edited by P. Haasen, V. Gerold and G. Kostorz (Pergamon, Oxford, 1980) p. 1503.
8. A. S. ARGON and S. TAKEUCHI, *Acta Metall.* **29** (1981) 1877.
9. B. DERBY and M. F. ASHBY, *ibid.* **35** (1987) 1349.
10. O. D. SHERBY, R. J. KLUNDT and A. K. MILLER, *Metall. Trans. A* **8A** (1977) 843.
11. D. McLEAN, *Trans. AIME* **22** (1968) 1193.
12. P. OSTROM and R. LAGNEBORG, *Res. Mechanica* **1** (1980) 59.
13. A. J. ARDELL and M. A. PRZSTUPA, *Mech. Mater.* **3** (1984) 319.
14. J. D. PARKER and B. WILSHIRE, *Phil. Mag.* **41A** (1980) 665.
15. H. E. EVANS and G. KNOWLES, *Acta Metall.* **25** (1977) 963.

16. O. AJAJA, *J. Mater. Sci.* **21** (1986) 3351.
17. M. E. KASSNER, A. K. MILLER and O. D. SHERBY, *Metall. Trans. A* **13A** (1982) 1977.
18. M. E. KASSNER, A. A. ZIAAI-MOAYYED and A. K. MILLER, *ibid.* **16A** (1985) 1069.
19. M. E. KASSNER, J. W. ELMER and C. J. ECHER, *ibid.* **17A** (1986) 2093.
20. O. AJAJA and A. J. ARDELL, *Scripta Metall.* **11** (1977) 1089.
21. *Idem, Phil, Mag.* **39** (1979) 65.
22. T. G. LANGDON, R. D. VASTAVA and P. YAVARI, in "Strength of Metals and Alloys," edited by P. Haasen, V. Gerold and G. Kostorz (Pergamon, Oxford, 1980) p. 271.
23. M. E. KASSNER and M. E. McMAHON, *Metall. Trans.* **18A** (1987) 835.
24. W. BLUM, A. ABSENGER and R. FEILHAUER, in "Strength of Metals and Alloys," edited by P. Haasen, V. Gerold and G. Kostorz (Pergamon, Oxford, 1980) p. 265.
25. S. KIKUCHI and A. YAMAGHUCHI, in "Strength of Metals and Alloys," edited by H. J. McQueen, J.-P. Bailon, J. I. Dickson, J. J. Jonas and M. G. Akben (Pergamon, Oxford, 1985) p. 899.
26. P. I. FERREIRA and R. G. STANG, *Acta Metall.* **31** (1983) 585.
27. T. J. GINTER and M. S. SOLIMAN, *Phil. Mag.* **50** (1984) 9.
28. C. M. YOUNG, S. L. ROBINSON and O. D. SHERBY, *Acta Metall.* **23** (1975) 633.
29. H. J. McQUEEN, J. K. SOLBERG, H. RYUM and E. NES, *Phil. Mag.* **60A** (1989) 473.
30. H. WIDERSICH, *J. Met.* **16** (1964) 423.
31. U. F. KOCKS, in "Strength of Metals and Alloys," edited by P. Haasen, V. Gerold and G. Kostorz (Pergamon, Oxford, 1980) p. 1661.
32. A. K. MUKHERJEE, in "Treatise on Materials Science and Technology," Vol. 6, edited by R. J. Arsenault (Academic, New York, 1975) p. 163.
33. S. TAKEUCHI and A. S. ARGON, *J. Mater. Sci.* **11** (1975) 1542.
34. T. J. GINTER and F. A. MOHAMED, *ibid.* **17** (1982) 2007.
35. V. K. SIKKA, H. NAHM and J. MOTEFF, *Mater. Sci. Eng.* **20** (1975) 55.
36. S. DAILY and C. N. AHLQUIST, *Scripta Metall.* **6** (1972) 95.
37. A. H. CLAUER, B. A. WILCOX and J. P. HIRTH, *Acta Metall.* **18** (1970) 381.
38. A. ORLOVA, M. PAHUTOVA and J. CADEK, *Phil. Mag.* **25** (1972) 865.
39. R. G. STANG, W. D. NIX and C. R. BARRETT, *Metall. Trans. A* **6A** (1975) 2065.
40. V. R. PARAMESWAREN, N. URABE and J. WEERTMAN, *Metall. Trans.* **2** (1971) 1233.
41. J. A. GORMAN, D. S. WOOD and T. VREELAND JR, *J. Appl. Phys.* **40** (1969) 833.
42. L. RAYMOND and J. E. DORN, *Trans. AIME* **230** (1964) 560.
43. C. R. BARRETT, W. D. NIX and O. D. SHERBY, *Trans. ASM* **59** (1966) 3.

Received 17 June 1988
and accepted 24 July 1989